92 Years of the Ising Model: A High Resolution Monte Carlo Study

IOP Conf. Series: Journal of Physics: Conf. Series **1012** (2018) 012002 doi:10.1088/1742-6596/1012/1/012002

92 Years of the Ising Model: A High Resolution Monte Carlo Study

Jiahao Xu[1], Alan M. Ferrenberg[2], David P. Landau[1]

1 Center for Simulational Physics, University of Georgia, Athens, GA 30602 USA
2 Information Technology Services and Department of Chemical, Paper & Biomedical Engineering, Miami University, Oxford, OH 45056 USA

E-mail: jiahaoxu@uga.edu, alan.ferrenberg@miamioh.edu, dlandau@physast.uga.edu

Abstract. Using extensive Monte Carlo simulations that employ the Wolff cluster flipping and data analysis with histogram reweighting and quadruple precision arithmetic, we have investigated the critical behavior of the simple cubic Ising model with lattice sizes ranging from 16^3 to 1024^3. By analyzing data with cross correlations between various thermodynamic quantities obtained from the same data pool, we obtained the critical inverse temperature $K_c = 0.221\,654\,626(5)$ and the critical exponent of the correlation length $\nu = 0.629\,912(86)$ with precision that improves upon previous Monte Carlo estimates.

1. Introduction

The Ising Model [1] has long played a special role in the theory of phase transitions and has served as a "fruit fly" model for testing new numerical and theoretical approaches. While Ising published the exact solution in 1-dim in 1925 [1] and Onsager the 2-dim version in 1944 [2], 3-dim Ising models have defied solution. Monte Carlo simulations [3], non-equilibrium relaxation Monte Carlo [4], Monte Carlo renormalization group [5, 6], field theoretic methods [7, 8] and high-temperature series expansions [9] have provided precise values for the location of the phase transition [10] and critical exponents, although the results did not all agree within the error bars. Simulations were insufficient to test Rosengren's "exact conjecture" for the critical temperature of the simple cubic Ising model [11]; moreover, Fisher showed that other "exact conjectures" gave quite similar values [12]. (For a nice review of results prior to 2002 see Ref. [10].)

Recent developments have renewed interest in the critical behavior of the 3d Ising model. The conformal bootstrap method provided precise estimates for the critical exponent ν [13, 14, 15], and Monte Carlo simulations [16, 17, 18] and tensor renormalization group theory with high-order singularity value decomposition [19] also yielded very precise results. Although Zhang claimed to have solved the 3d Ising model exactly [20], convincing arguments showed that his solution was incorrect [21, 22, 23].

We now present new results of high-precision Monte Carlo simulations of critical behavior of the simple cubic Ising model, analyzed using histogram reweighting techniques [24, 25], cross correlation analysis [26, 27] and finite-size scaling methods [28, 29, 30, 31].

2. Model and methods

2.1. Three-dimensional Ising model

We have considered the simple cubic, ferromagnetic Ising model with nearest-neighbor interactions on $L \times L \times L$ lattices with periodic boundary conditions. Each of the lattice sites i has a spin, $\sigma_i = \pm 1$ which interact with Hamiltonian

$$\mathcal{H} = -J \sum_{\langle i,j \rangle} \sigma_i \sigma_j, \tag{1}$$

where $\langle i, j \rangle$ denotes distinct pairs of nearest-neighbors and J is the interaction constant. The dimensionless energy E is

$$E = -\sum_{\langle i,j \rangle} \sigma_i \sigma_j. \tag{2}$$

The dimensionless coupling constant $K = J/k_B T$ will be useful for discussing critical behavior.

2.2. Monte Carlo algorithm

We sampled states using the Wolff cluster flipping algorithm [32] in which single clusters are grown and flipped sequentially. Clusters are created by drawing bonds to all nearest neighbors of the growing cluster with probability

$$p = 1 - e^{-2K\delta_{\sigma_i \sigma_j}} \tag{3}$$

Random numbers were produced using the Mersenne Twister generator [33]. No difference was discernible between data obtained using 32-bit and 53-bit versions. Simulations were performed at $K_0 = 0.221\,654$ (the estimate for the critical inverse temperature K_c by MCRG analysis [6], also used in an earlier, high resolution Monte Carlo study [3]). Lattice sizes were in the range $16 \leq L \leq 1024$, and measurements were taken for each run after 2×10^5 Wolff steps were discarded for equilibrium. Even for the largest lattice, $L = 1024$, the energy had reached equilibrium by $130,000$ cluster steps, and the simulation was then run at least another ten times the equilibrium relaxation time before data accumulation began. We performed 6,000 to 12,000 runs of 5×10^6 measurements for each L using a total of around 2×10^7 CPU core hours and producing more than 5TB data.

2.3. Methods of analysis

To locate the peaks in response functions precisely we used histogram reweighting [24, 25] to transform a probability distribution measured at one coupling to one at an adjacent value of coupling. After N configurations are generated at inverse temperature K_0 with a probability proportional to the Boltzmann weight, $\exp(-K_0 E)$, the probability of simultaneously observing the system with total (dimensionless) energy E and total magnetization M is estimated,

$$P_{K_0} = \frac{1}{Z(K_0)} W(E, M) \exp(K_0 E) \approx H(E, M)/N, \tag{4}$$

where $Z(K_0)$ is the partition function and $H(E, M)$ is the measured histogram of states. The (estimated) probability distribution for arbitrary K is then

$$P_K(E, M) \approx \frac{H(E, M) e^{\Delta K E}}{\sum H(E, M) e^{\Delta K E}}, \tag{5}$$

where $\Delta K = K_0 - K$ and the average value of any function of E and M, $f(E, M)$,

$$\langle f(E, M) \rangle_K = \sum_{E,M} f(E, M) P_K(E, M) \tag{6}$$

Ferrenberg and Landau [3] showed that the critical exponent ν of the correlation length can be estimated more precisely from Monte Carlo simulation data if multiple quantities, including traditional quantities which still have the same critical properties, are included. The logarithmic derivative of any power of the magnetization

$$\frac{\partial \ln \langle |m|^i \rangle}{\partial K} = \frac{1}{\langle |m|^i \rangle} \frac{\partial \langle |m|^i \rangle}{\partial K} = \frac{\langle |m|^i E \rangle}{\langle |m|^i \rangle} - \langle E \rangle, \tag{7}$$

for $i = 1, 2, ...$, can yield an estimate for ν. We also included (reduced) magnetization cumulants U_{2i} [34] defined by

$$U_{2i} = 1 - \frac{\langle |m|^{2i} \rangle}{3 \langle |m|^i \rangle^2}, \quad i = 1, 2, 3, ... \tag{8}$$

whose derivatives with respect to K can also be used to estimate ν. The inverse critical temperature $K_c(L)$ can be estimated from the locations of the peaks in the above quantities as well as the specific heat

$$C = K^2 L^{-d} (\langle E^2 \rangle - \langle E \rangle^2), \tag{9}$$

the derivative of $|m|$ with respect to K,

$$\frac{\partial \langle |m| \rangle}{\partial K} = \langle |m| E \rangle - \langle |m| \rangle \langle E \rangle, \tag{10}$$

the finite-lattice susceptibility,

$$\chi' = K L^d (\langle |m|^2 \rangle - \langle |m| \rangle^2), \tag{11}$$

and the zero of the fourth-order energy cumulant

$$Q_4 = 1 - \frac{\langle (E - \langle E \rangle)^4 \rangle}{3 \langle (E - \langle E \rangle)^2 \rangle^2}. \tag{12}$$

Note that Eq. (11) is for the finite-lattice susceptibility, not the "true" susceptibility calculated from the variance of m, $\chi = K L^d (\langle m^2 \rangle - \langle m \rangle^2)$ which has no peak for finite L. (For long runs, $\langle m \rangle = 0$ for $H = 0$ so that any peak in χ is merely due to finite run length.) All quantities were calculated using the GCC Quad-Precision Math Library (quadruple, 128 bit) precision.

The critical behavior of a system near a 2nd order transition can be extracted from the size dependence of the singular part of the free energy density [28, 29, 30, 31]. As a function of L (linear dimension) and T (temperature) as variables, the free energy of a system is described by the finite size scaling (FSS) ansatz,

$$F(L, T) = L^{-(2-\alpha)/\nu} \mathcal{F}(\varepsilon L^{1/\nu}, h L^{(\gamma+\beta)/\nu}), \tag{13}$$

where $\varepsilon = (T - T_c)/T_c$ (T_c is the infinite-lattice critical temperature), h is the magnetic field, and the critical exponents α, β, γ and ν are the infinite lattice values. Various thermodynamic properties can be determined from Eq. (13) and have corresponding scaling forms, e.g.,

$$m = L^{-\beta/\nu} \mathcal{M}^0(\varepsilon L^{1/\nu}), \tag{14}$$

$$\chi = L^{\gamma/\nu} \chi^0(\varepsilon L^{1/\nu}), \tag{15}$$

$$C = L^{\alpha/\nu} \mathcal{C}^0(\varepsilon L^{1/\nu}), \tag{16}$$

where $\mathcal{M}^0(x)$, $\chi^0(x)$ and $\mathcal{C}^0(x)$ are scaling functions. Because we are interested in zero-field properties ($h = 0$), x is the only relevant thermodynamic variable. Then, for finite L, e.g. the specific heat peak occurs where the scaling function $\mathcal{C}^0$ is maximum, i.e., when

$$\left.\frac{\partial \mathcal{C}^0(x)}{\partial x}\right|_{x=x^*} = 0. \tag{17}$$

The temperature corresponding to the peak is the finite-lattice "transition" temperature $T_c(L)$, on the condition $x = x^*$ which varies with L asymptotically as

$$T_c(L) = T_c + T_c x^* L^{-1/\nu}. \tag{18}$$

The FSS ansatz is valid only for sufficiently large L and T sufficiently close to T_c. Corrections to scaling and finite-size scaling terms appear for smaller systems and temperatures away from T_c due to: irrelevant scaling fields which can be expressed in terms of an exponent θ, e.g. $a_1\varepsilon^\theta + a_2\varepsilon^{2\theta} + \cdots$, and others due to the non-linear scaling fields, e.g. $b_1\varepsilon^1 + b_2\varepsilon^2 + \cdots$. The correction terms can then be expressed by: $a_1 L^{-\theta/\nu} + a_2 L^{-2\theta/\nu}$ and $b_1 L^{-1/\nu} + b_2 L^{-2/\nu}$. Including correction terms, the estimate for the inverse critical coupling $K_c(L)$ becomes

$$K_c(L) = K_c + A_0 L^{-1/\nu}(1 + A_1 L^{-\omega_1} + A_2 L^{-\omega_2} + \cdots). \tag{19}$$

We first estimate the critical exponent ν and then insert it into Eq. (19), so that there is one less unknown parameter to do the non-linear fit to Eq. (19). To do this we can use the critical scaling form without the prior knowledge of the transition coupling K_c

$$\left.\frac{\partial U_{2i}}{\partial K}\right|_{\max} = U_{i,0} L^{1/\nu}(1 + a_1 L^{-\omega_1} + a_2 L^{-\omega_2} + \cdots) \tag{20}$$

$$\left.\frac{\partial \ln \langle |m|^i \rangle}{\partial K}\right|_{\max} = D_{i,0} L^{1/\nu}(1 + a_1 L^{-\omega_1} + a_2 L^{-\omega_2} + \cdots) \tag{21}$$

Once ν is determined from the fit of Eq. (20) and Eq. (21), we can estimate the critical inverse temperature K_c with a fixed value of ν. K_c can also be estimated from Binder's 4th order cumulant crossing technique [34]. As $L \to \infty$, the fourth-order magnetization cumulant $U_4 \to 0$ for $K < K_c$ and $U_4 \to 2/3$ for $K > K_c$. U_4 can be plotted as a function of K for different lattice sizes, and the location of the intersections between curves for the two lattice sizes is given by

$$K_{\text{cross}}(L, b) = K_c + a_1 L^{-1/\nu-\omega_1}\left(\frac{b^{-\omega_1} - 1}{b^{1/\nu} - 1}\right) + a_2 L^{-1/\nu-\omega_2}\left(\frac{b^{-\omega_2} - 1}{b^{1/\nu} - 1}\right) + \cdots$$

where L is the size of the smaller lattice, $b = L'/L$ is the ratio of two lattice sizes, and ω_1, ω_2 are correction exponents in the finite-size scaling formulation.

Ideally, each configuration only depends on the previous configuration, but, in practice, it is likely to be correlated to earlier configurations. The correlation decays with separation in Monte Carlo time, but fluctuations appear smaller than they should be. To deal with this issue, we can consider blocks of the original data, and use jackknife resampling [35].

An important advance by Weigel and Janke [26, 27] was the seminal observation that cross correlation between different quantities could lead to systematic bias in the estimates of critical quantities extracted from the data. For a set of n measurements of a random variable $\mathbf{x} = (x_1, x_2, \cdots, x_n)$, and an estimator $\hat{\theta} = f(\mathbf{x})$, the Jackknife estimate of the value and error of $\hat{\theta}$ is found by leaving out one measurement at a time. We define the jackknife average, x_i^J by,

$$x_i^J = \frac{1}{n-1}\sum_{j \neq i} x_j, \tag{22}$$

where $i = 1, 2, \cdots, n$, so x_i^J is the average of all the x values except x_i. Similarly, we define

$$\hat{\theta}_i^J = f(x_i^J). \tag{23}$$

The jackknife estimate of $\hat{\theta} = f(\mathbf{x})$ is the average of $\hat{\theta}_i^J$, i.e.

$$\bar{\theta} = \frac{1}{n}\sum_{i=1}^{n}\hat{\theta}_i^J = \frac{1}{n}\sum_{i=1}^{n} f(x_i^J), \tag{24}$$

and the jackknife error $\sigma(\hat{\theta})$, is given by,

$$\sigma(\hat{\theta}) = \left[\frac{n-1}{n}\sum_{i=1}^{n}(\hat{\theta}_i^J - \bar{\theta})^2\right]^{1/2}. \tag{25}$$

In general there can be multiple adjacent elements in each block, and significant cross correlations may exist between estimates $\hat{\theta}^{(k)}$ and $\hat{\theta}^{(l)}$ from the same original time-series data, To reduce these effects, we calculated the jackknife covariance matrix $\mathbf{G} \in \mathbb{R}^{m\times m}$ [35]. For a number of estimates $\hat{\theta}^{(k)}$, the r^{th} row, c^{th} column entry of matrix $\mathbf{G}$ is given by,

$$\mathbf{G}_{rc}(\hat{\theta}) = \frac{n-1}{n}\sum_{i=1}^{n}(\hat{\theta}_i^{J,(r)} - \bar{\theta}^{(r)})(\hat{\theta}_i^{J,(c)} - \bar{\theta}^{(c)}). \tag{26}$$

The m different estimates $\hat{\theta}^{(k)}(k = 1, 2, ..., m)$ for the same parameter $\hat{\theta}$, should have the same expectation value. So the estimated value for $\hat{\theta}$ can be determined by a linear combination,

$$\bar{\theta} = \sum_{k=1}^{m}\alpha_k\hat{\theta}^{(k)}. \tag{27}$$

where $\sum_k \alpha_k = 1$. Based on the cross correlation analysis from Ref. [26, 27], with the optimal choice for the weights, the variance can be expressed by,

$$\sigma^2(\hat{\theta}) = \frac{1}{\sum_{k=1}^{m}\sum_{l=1}^{m}[\mathbf{G}(\hat{\theta})^{-1}]_{kl}}. \tag{28}$$

At our level of resolution the finite precision of the pseudorandom number generator and the numbers that can be stored in memory become relevant. When the Wolff algorithm probability of adding a spin to the cluster is converted to a 32-bit unsigned number for comparison with a pseudorandom number generated in the simulation, it is truncated due to finite precision. When reconverted back into a value of K the result differs from 0.221 654 in the 10th decimal place. For the largest L, this is only a factor of 20 smaller than the statistical error. Simulations with a 53-bit pseudorandom number generator showed that this is not significant for our analysis, but for future studies of larger systems and/or higher precision, a 32-bit random number generator might not suffice. We also used the corrected, effective K_0 instead of 0.221654 and for $L = 1024$ we used the multiple-histogram method [25] to combine results for the 32 and 53-bit pseudorandom number generators.

Comparisons of results from Wolff cluster flipping runs and Metropolis single spin-flip runs for $L = 32$ showed no differences. The Wolff cluster simulation for L=32 was repeated using the MRG32K3A random number generator from Pierre L'Ecuyer, "Combined Multiple Recursive Random Number Generators", Operations Research, 47, 1 (1999), 159-164. The locations and values of the maxima in all quantities agreed, to within the error bars, as those from the Metropolis simulations and the Wolff simulations with the Mersenne Twister. Hence the problems found by Ferrenberg et al. [36] using other random number generators were not noticeable here.

Table 1. Estimates for ν with: one fixed correction exponent $\omega_1 = 0.83$, two fixed exponents $\omega_1 = 0.83$, $\omega_2 = 4$, and three fixed exponents $\omega_1 = 0.83$, $\omega_2 = 4$, $\omega_3 = 1.6$ as a function of $L_{\min}$.

$L_{\min}$	$\nu(\omega_1$ fixed)	$\nu(\omega_{1,2}$ fixed)	$\nu(\omega_{1,2,3}$ fixed)
16	0.631 814(18)	0.630 806(30)	0.630 072(45)
24	0.631 046(26)	0.630 513(40)	0.630 049(57)
32	0.630 722(33)	0.630 241(55)	0.629 980(77)
48	0.630 350(48)	0.630 278(78)	0.629 99(11)
64	0.630 319(62)	0.630 21(11)	0.630 06(15)
80	0.630 285(78)	0.630 10(15)	0.629 93(21)
96	0.630 25(10)	0.629 93(18)	0.629 90(29)
112	0.630 14(13)	0.630 01(17)	0.629 93(18)
128	0.630 04(15)	0.630 04(15)	0.629 84(22)
144	0.629 85(18)	0.629 85(18)	0.629 96(26)

3. Results

3.1. Finite-size scaling analysis

The conformal bootstrap [13, 14] gives a theoretical prediction for the confluent correction exponents,

$$\omega_1 = 0.8303(18), \quad \omega_2 \approx 4. \tag{29}$$

and the correction term corresponding to the non-linear scaling fields is [37],

$$\omega_3 = 1/\nu \tag{30}$$

Thus, the fitting model for the peak value of quantity X is,

$$X_{\max} = X_0 L^{1/\nu}(1 + a_1 L^{-\omega_1} + a_2 L^{-\omega_2} + a_3 L^{-\omega_3}) \tag{31}$$

We analyzed the data fitting model Eq. (31) using between one and three correction terms with fixed powers $\omega_1 = 0.83$, $\omega_2 = 4$, $\omega_3 = 1.6$. By calculating the covariance matrix and doing the cross-correlation analysis, we give estimates for ν in Table 1 where the minimum lattice size included in the analysis, $L_{\min}$, is eliminated one by one. With three correction exponents, two for confluent corrections ($\omega_1 = 0.83$, $\omega_2 = 4$) and one for the non-linear scaling fields ($\omega_3 = 1.6$), the estimate for the critical exponent ν shows statistical fluctuations; but the value for ν was estimated by taking the average of ν obtained from fits for different $L_{\min}$ and the error estimated with the jackknife method on estimates of ν from the analysis using different ranges of relatively large $L_{\min}$. Using values of $L_{\min}$ from 80 to 144, we find

$$\nu = 0.629\,912(86). \tag{32}$$

Since higher order terms like $a_{1,2}L^{-2\omega_1} + \cdots$ could be present and larger than the higher order confluent corrections, we repeated the analysis using these higher order corrections instead. The results for the asymptotic values of the critical temperature and exponent were essentially identical. Thus, either the higher order terms have small prefactors or we do not have sufficient resolution to differentiate their contribution from those of higher order confluent corrections.

To estimate the critical coupling K_c, we fitted the locations of the peak of the multiple quantities using between one and three fixed correction exponents, $\omega_1 = 0.83$, $\omega_2 = 4$, $\omega_3 = 1.6$, to the fitting model Eq. (33),

$$K_c(L) = K_c + A_0 L^{-1/\nu}(1 + A_1 L^{-\omega_1} + A_2 L^{-\omega_2} + A_3 L^{-\omega_3}). \tag{33}$$

Table 2. Fitted values for K_c with: (left column) one correction term (fixed exponent $\omega_1 = 0.83$); (center column) two correction terms (fixed exponents $\omega_1 = 0.83$, $\omega_2 = 4$; and (right column) three correction terms (fixed exponents $\omega_1 = 0.83$, $\omega_2 = 4$, $\omega_3 = 1.6$) as a function of $L_{\min}$.

$L_{\min}$	K_c(1 fixed ω)	K_c(2 fixed ω)	K_c(3 fixed ω)
16	0.221 654 656 2(10)	0.221 654 639 3(11)	0.221 654 625 7(21)
24	0.221 654 638 8(11)	0.221 654 630 8(12)	0.221 654 625 7(24)
32	0.221 654 634 3(11)	0.221 654 630 7(12)	0.221 654 625 3(32)
48	0.221 654 630 7(12)	0.221 654 630 5(12)	0.221 654 623 2(30)
64	0.221 654 628 4(13)	0.221 654 628 4(13)	0.221 654 623 4(60)
80	0.221 654 627 5(14)	0.221 654 627 5(15)	0.221 654 625 0(75)
96	0.221 654 626 0(17)	0.221 654 626 0(16)	0.221 654 627 9(97)
112	0.221 654 625 9(18)	0.221 654 626 0(18)	0.221 654 625 0(49)
128	0.221 654 625 8(21)	0.221 654 625 8(21)	0.221 654 626 3(48)
144	0.221 654 627 0(25)	0.221 654 627 0(25)	0.221 654 627 1(34)

The results for K_c are shown in Table 2.

The fluctuation of K_c when $L_{\min} \leq 80$ is larger than when $L_{\min} \geq 80$ and finite-size effects diminish for larger L. From the average of K_c for $L_{\min} = 80$ to 144 we estimate $K_c = 0.221\,654\,626\,2$. Likewise, a jackknife analysis has been done on the estimates for K_c which are obtained from the three correction terms analysis. From values of $L_{\min}$ from 80 to 144 we estimate $K_c = 0.221\,654\,626\,2(23)$ whereas for $L_{\min} = 16$ to 144, $K_c = 0.221\,654\,625\,5(42)$. Therefore, we conclude from the finite size scaling analysis, with conservative error bars, that

$$K_c = 0.221\,654\,626(5). \tag{34}$$

As seen in Fig. 2, effects of higher order correction terms are clearly visible.

3.2. Crossing technique of the 4th order magnetization cumulant

As the lattice size $L \to \infty$, the fourth-order magnetization cumulant $U_4 \to 0$ for $K < K_c$ and $U_4 \to 2/3$ for $K > K_c$. For large enough lattice sizes, curves for U_4 cross as a function of inverse temperature at a "fixed point" U^*, and the location of the crossing "fixed point" is K_c. Because of finite-size correction terms, not all curves cross at a common intersection. The locations of the cumulant crossings have been fitted to Eq. (22) with two correction terms. The critical coupling appears to be stable if $L_{\min} \geq 96$ and the average of K_c values for $L_{\min} \geq 96$ yields

$$K_c = 0.221\,654\,628(2) \tag{35}$$

3.3. Discussion

The combination of an efficient, cluster-flipping Monte Carlo algorithm, high statistics simulations, histogram reweighting, and a cross-correlation jackknife analysis enables the high resolution of the results presented above. In Fig. 3, we show the results of our Monte Carlo study as well as other high-resolution simulations estimates for ν and K_c. The boxes represent the quoted error bars in both ν and K_c assuming independent errors.

Our estimate $\nu = 0.629\,912(86)$ is consistent (i.e. within the error bars) with the recent conformal bootstrap result of Kos et al. [15], as well as that from an older work by El-Showk et al. [14]. Also, our result agrees well with the Monte Carlo result of Hasenbusch [16] but is lower

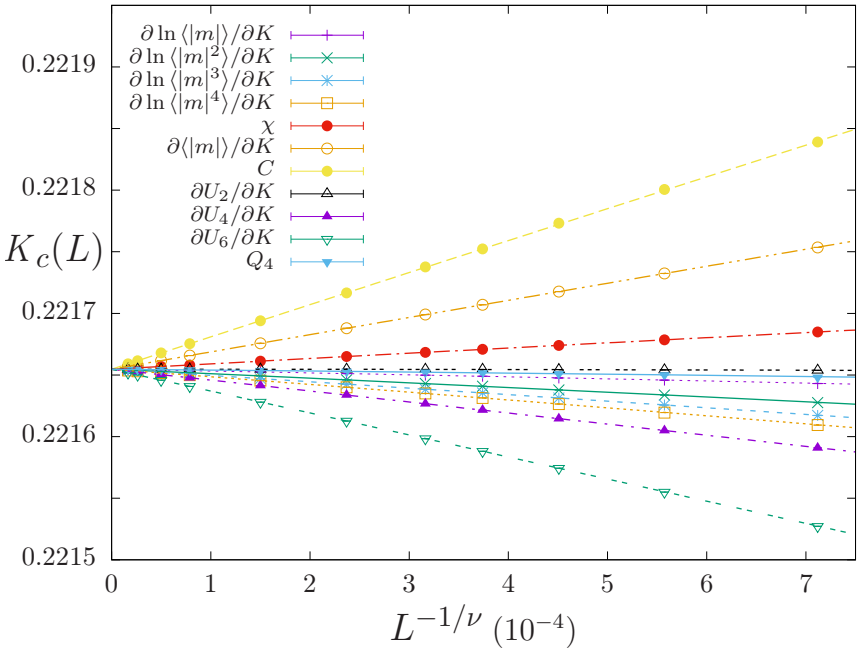

Figure 1. Size dependence of the finite-lattice effective critical temperatures estimated from $L = 96$ to 1024.

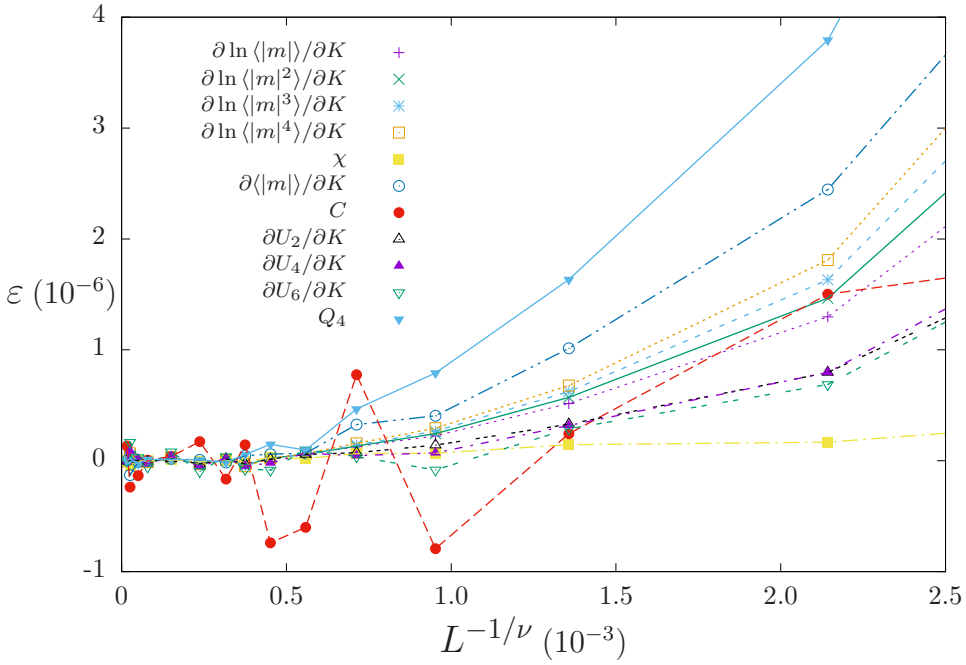

Figure 2. Size dependence of the residual difference between measured K_c and fitted values including one correction term.

Table 3. Comparison of our results for the critical coupling K_c and the critical exponents ν, γ with other recently obtained values. Numbers marked with * are calculated by Fisher's scaling law $\gamma = \nu(2-\eta)$, and the error estimates assume that ν an η are independent and uncorrelated.

Method	K_c	ν	γ
conformal bootstrap [15]		0.629 971(4)	1.237 075(8)*
MC [27]	0.221 657 03(85)	0.630 0(17)	1.240 9(62)*
MC [16]	0.221 654 63(8)	0.630 02(10)	1.237 19(21)*
MC [17]	0.221 654 604(18)		
tensor RG [19]	0.221 654 555 5(5)		
Our results (no fit assumptions), MC	0.221 654 630(7)	0.629 60(15)	1.236 41(45)
Our results (constrained fits), MC	0.221 654 626(5)	0.629 912(86)	1.236 94(31)
Our results (cumulant crossings), MC	0.221 654 628(2)		

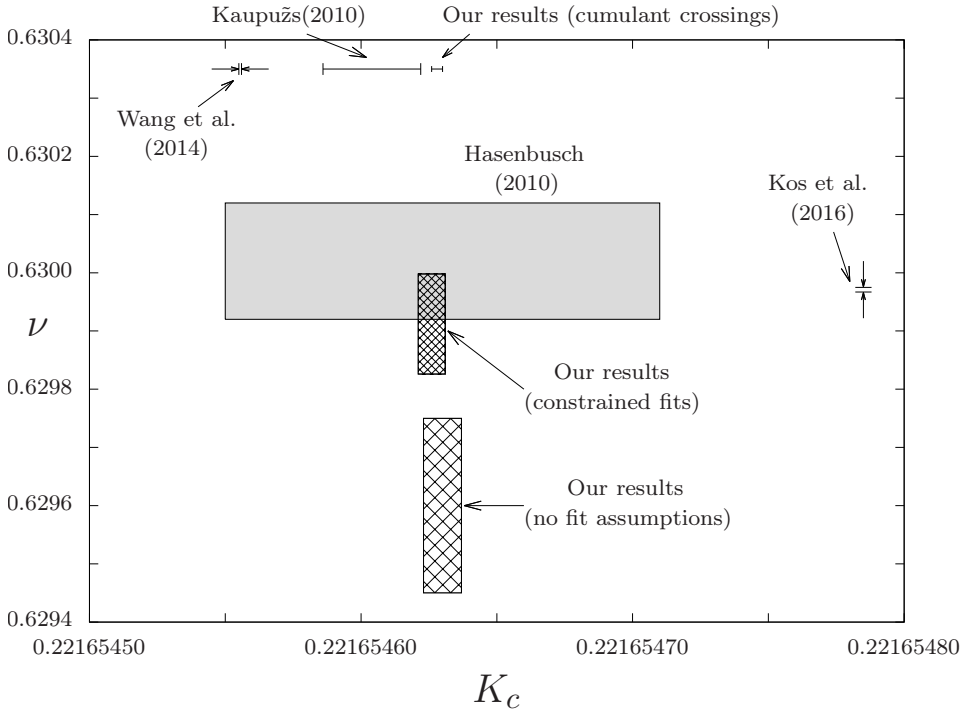

Figure 3. High-resolution estimates for K_c and ν obtained using different methods

than that of Weigel and Janke [27]; however, within the respective error bars there is agreement although we have substantially higher precision than either of these previous studies. Our system sizes and statistics are substantially greater than those used by Weigel and Janke and Hasenbusch examined the behavior of the ratio of partition functions Z_a/Z_p, and the second moment correlation length over the linear lattice size ξ_2/L so the methodologies differ. Our estimate for K_c differs from that obtained by Kaupužs et al [17] using a parallel Wolff algorithm by an amount that is slightly outside the error bars. Somewhat perplexingly, they were able to fit their data to two rather different values of ν, so no comparison of critical exponents is possible. The recent tensor renormalization group result for K_c [19] disagrees with our result by many times the respective error bars.

4. Conclusion

We have studied a 3d Ising model with the Wolff cluster flipping algorithm, histogram reweighting, and finite size scaling including cross-correlations using quadruple precision arithmetic for the analysis. Using a wide range of system sizes, with the largest containing more than 10^9 spins, and including corrections to scaling, we have obtained results for K_c, ν, and γ that are comparable in precision to those from the latest theoretical predictions and can provide independent verification of the predictions from those methods. Our values provide further numerical evidence that none of the purported "exact" values are correct. To within error bars we obtain the same value for the critical exponent ν as that predicted by the conformal bootstrap; however, our estimate for the critical temperature K_c does not agree with that from the tensor renormalization group.

As computer power increases, new sources of error must be taken into account. To improve precision more stringent tests of the random number generator and much greater statistics for much larger lattice sizes will be needed.

Acknowledgments

We thank Dr. M. Weigel and Dr. S.-H. Tsai for valuable discussions. Computing resources were provided by the Georgia Advanced Computing Resource Center, the Ohio Supercomputing Center, and the Miami University Computer Center.

References

[1] Ising E 1925 *Z. Phys.* **31** 253–258
[2] Onsager L 1944 *Phys. Rev.* **65** 117–149
[3] Ferrenberg A M and Landau D P 1991 *Phys. Rev. B* **44** 5081
[4] Ozeki Y and Ito N 2007 *J. Phys. A: Math. Theor.* **40** R149–R203
[5] Blöte H W J, Heringa J R, Hoogland A, Meyer E W and Smit T S 1996 *Phys. Rev. Lett.* **76** 2613–2616
[6] Pawley G S, Swendsen R H, Wallace D J and Wilson K G 1984 *Phys. Rev. B* **29** 4030–4040
[7] Guida R and Zinn-Justin J 1998 *J. Phys. A* **31** 8103
[8] Pogorelov A A and Suslov I M 2008 *J. Exp. Theor. Phys.* **106** 1118
[9] Butera P and Comi M 2005 *Phys. Rev. B* **72** 014442
[10] Pelissetto A and Vicari E 2002 *Phys. Rep.* **368** 549
[11] Rosengren A 1986 *J. Phys. A: Math. Gen.* **19** 1709
[12] Fisher M E 1995 *J. Phys. A: Math. Gen.* **28** 6323
[13] El-Showk S, Paulos M F, Poland D, Rychkov S, Simmons-Duffin D and Vichi A 2012 *Phys. Rev. D* **86** 025022
[14] El-Showk S, Paulos M F, Poland D, Rychkov S, Simmons-Duffin D and Vichi A 2014 *J. Stat. Phys.* **157** 869
[15] Kos F, Poland D, Simmons-Duffin D and Vichi A 2016 *J. High Energ. Phys.* **2016** 36
[16] Hasenbusch M 2010 *Phys. Rev. B* **82** 174433
[17] Kaupužs J, Rimsans J and Melnik R V N 2011 *Ukr. J. Phys.* **56** 845
[18] Kaupužs J, Melnik R V N and Rimsans J 2014 *ArXiv e-prints* (*Preprint* 1407.3095)
[19] Wang S, Xie Z Y, Chen J, Normand B and Xiang T 2014 *Chin. Phys. Lett.* **31** 070503
[20] Zhang Z 2007 *Phil, Mag.* **87** 5309
[21] Wu F, McCoy B M, Fisher M E and Chayes L 2008 *Phil. Mag.* **88** 3093–3095
[22] Wu F, McCoy B M, Fisher M E and Chayes L 2008 *Phil. Mag.* **88** 3103–3103
[23] Fisher M E and Perk J H H 2016 *Phys. Lett. A* **380** 1339 – 1340
[24] Ferrenberg A M and Swendsen R H 1988 *Phys. Rev. Lett.* **61** 2635
[25] Ferrenberg A M and Swendsen R H 1989 *Phys. Rev. Lett.* **63** 1195
[26] Weigel M and Janke W 2009 *Phys. Rev. Lett.* **102** 100601
[27] Weigel M and Janke W 2010 *Phys. Rev. E* **81** 066701
[28] Fisher M E 1971 *Critical Phenomena* (New York: Academic Press) pp 1–98
[29] Fisher M E and Barber M N 1972 *Phys. Rev. Lett* **28** 1516
[30] Barber M N 1983 *Phase Transitions and Critical Phenomena* vol 8 (New York: Academic Press) pp 146–266
[31] Privman V 1990 *Finite-Size Scaling and Numerical Simulation* (Singapore: World Scientific)
[32] Wolff U 1989 *Phys. Rev. Lett.* **62** 361–364
[33] Matsumoto M and Nishimura T 1998 *ACM Trans. Model. Comput. Simul.* **8** 3–30 ISSN 1049-3301
[34] Binder K 1981 *Z. Phys. B* **43** 119

[35] Efron B and Tibshirani R J 1993 *An Introduction to the Bootstrap* (New York: Chapman and Hall)
[36] Ferrenberg A, Landau D P and Wong Y 1992 *Phys. Rev. Lett.* **69** 3382–3384
[37] Aharony A and Fisher M E 1983 *Phys. Rev. B* **27** 4394–4400